Cyclostrophic winds from the Visible and Infrared Thermal Imaging Spectrometer temperature sounding: A preliminary analysis

Arianna Piccialli, Dmitry V. Titov, Davide Grassi, Igor V. Khatuntsev, Pierre Drossart, Giuseppe Piccioni, Alessandra Migliorini

Cyclostrophic winds from the Visible and Infrared Thermal Imaging Spectrometer temperature sounding: A preliminary analysis

A. Piccialli,[1] D. V. Titov,[1,2] D. Grassi,[3] I. Khatuntsev,[2] P. Drossart,[4] G. Piccioni,[5] and A. Migliorini[5]

Received 25 February 2008; accepted 25 July 2008; published 22 October 2008.

[1] Visible and Infrared Thermal Imaging Spectrometer (VIRTIS) onboard the Venus Express spacecraft has been operating since April 2006 providing new observations of the temperature structure of Venus mesosphere (60–95 km). Zonal winds in the middle atmosphere of Venus have been retrieved from VIRTIS temperature profiles using the cyclostrophic approximation. The wind field is characterized by three main features: (1) a midlatitude jet connected to the thermal feature known as the cold collar; the jet reaches a maximum speed of 80–90 ± 10 m/s near the cloud top (~70 km altitude) at 50°S latitude; (2) a strong decrease of wind from 60°S toward the pole reaching zero velocity at ~70°S; and (3) the decrease of the wind above the jet with increasing altitude. Local time dependence of the temperature and wind field has been analyzed. Temperatures show at cloud tops a cooling of ~15 K during the night which propagates also on the zonal wind field. Comparison with cloud-tracked winds from Venus Monitoring Camera images indicates a first-order agreement.

Citation: Piccialli, A., D. V. Titov, D. Grassi, I. Khatuntsev, P. Drossart, G. Piccioni, and A. Migliorini (2008), Cyclostrophic winds from the Visible and Infrared Thermal Imaging Spectrometer temperature sounding: A preliminary analysis, *J. Geophys. Res.*, *113*, E00B11, doi:10.1029/2008JE003127.

1. Introduction

[2] Early observations showed that the Venus atmosphere has two different dynamic regimes. In the thermosphere above ~100 km diurnal temperature gradients force global solar-antisolar circulation [*Bougher et al.*, 1997; *Lellouch et al.*, 1997]. Troposphere and mesosphere (0–100 km) are involved in the retrograde almost purely zonal motion with maximum wind speed of about 100 m/s at the cloud tops, called superrotation. The physical mechanisms that maintain this global regular motion are still not known [*Schubert*, 1983; *Gierasch et al.*, 1997; *Schubert et al.*, 2007]. *Leovy* [1973] was first to notice that on a slowly rotating planet, where Coriolis force is negligible, the global zonal circulation is a result of local balance of pressure gradient and centripetal force which is called cyclostrophic balance. The thermal wind equation that describes this balance relates vertical shear of zonal wind to latitudinal temperature gradient on a constant pressure surface [*Leovy*, 1973; *Schubert*, 1983]. Although the cyclostrophic balance seems to clearly describe the observed state of Venus superrotation, it does not explain what originally brought the atmosphere to this state or which mechanisms maintain the vertical wind shear.

[3] Temperature structure of the Venus mesosphere was sounded remotely by radio occultation and thermal emission radiometry and spectroscopy on the Pioneer Venus and Venera-15 orbiters [*Seiff*, 1983; *Taylor et al.*, 1983; *Seiff et al.*, 1985; *Lellouch et al.*, 1997; *Zasova et al.*, 2007]. The mesospheric temperature field showed two remarkable peculiarities. Temperatures above ~75 km monotonically increase from equator to pole thus creating positive latitudinal temperature gradient at constant pressure level. Inside the upper cloud layer (60–75 km) the trend reverses and temperature field forms a bulge of cold air at 60°–80° latitude which was called "cold collar."

[4] The measured temperatures were used to derive zonal wind field using the cyclostrophic approximation [*Chub and Yakovlev*, 1980; *Seiff*, 1983; *Newman et al.*, 1984; *Limaye*, 1985; *Roos-Serote et al.*, 1995; *Zasova et al.*, 2007]. These studies constrained the winds in the poorly explored region of transition to the solar-antisolar thermospheric circulation. The main features of the cyclostrophic wind field are (1) the presence of strong midlatitude jet centered at ~50° latitude and ~70 km altitude and (2) the decrease of zonal wind with altitude above the cloud top. This behavior is governed by the latitudinal temperature contrasts. In the midlatitudes the atmosphere is accelerated at the cloud level by negative latitudinal gradient of temperature associated with the cold collar. Above the cloud tops on the contrary positive temperature gradient forces the winds to fade out with altitude. The cyclostrophic balance was found to break above 70–75 km in high (>70°) and low

[1]Max Planck Institute for Solar System Research, Katlenburg-Lindau, Germany.
[2]Space Research Institute, Moscow, Russia.
[3]Istituto di Fisica dello Spazio Interplanetario, INAF, Rome, Italy.
[4]LESIA, Observatoire de Paris, Meudon, France.
[5]Istituto di Astrofisica Spaziale e Fisica Cosmica, INAF, Rome, Italy.

0148-0227/08/2008JE003127

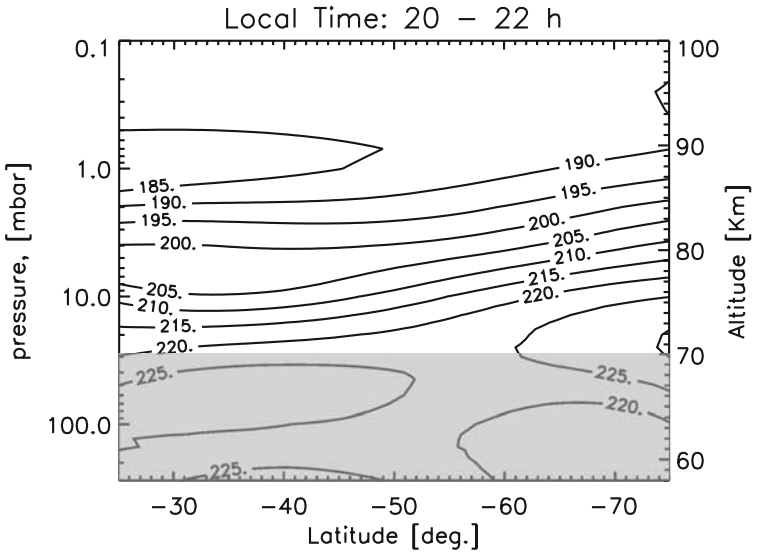

Figure 1. Contours of temperature field averaged over the range 2000–2200 LT for the VIRTIS-M orbit VI0072. Contour interval is 5 K. In gray the cloud layer is represented schematically.

(<40°) latitudes. Here the latitudinal temperature gradient cannot provide centripetal force for the air parcels involved in the zonal motion. The magnitude of the midlatitude jet changes from ~160 m/s in the work by *Newman et al.* [1984] to ~100 m/s in the work by *Zasova et al.* [2007]. Position of the jet core showed meandering in the latitude range of 45°–65° and altitudes of 65–70 km. *Zasova et al.* [2007] also reported about diurnal and semidiurnal harmonics present in the thermal wind pattern derived from Venera-15 data.

[5] Since April 2006, Venus Express carries out systematic remote sensing observations of the Venus mesosphere using both radio occultation and thermal emission spectroscopy techniques [*Svedhem et al.*, 2007; *Häusler et al.*, 2006; *Drossart et al.*, 2007]. Polar orbit of the satellite allows the experiments to achieve full latitude coverage and especially focus of the southern hemisphere poorly studied in the earlier missions [*Titov et al.*, 2006]. Here we present the first results of calculations of the cyclostrophic wind field from the temperature sounding by VIRTIS experiment [*Grassi et al.*, 2008].

2. Temperature Field in the Mesosphere

[6] Visible and Infrared Thermal Imaging Spectrometer (VIRTIS) is one of the experiments on board of Venus Express. It consists of two channels. VIRTIS-M is an imaging spectrometer with moderate spectral resolution (R~200) and high spatial resolution (0.25 mrad) operating in the spectral ranges 0.25–1 μm and 1–5 μm. VIRTIS-H is a high-resolution spectrometer (R~1200) operating in the spectral range 1.84–4.99 μm [*Drossart et al.*, 2007; *Piccioni et al.*, 2008]. VIRTIS-M acquires thermal emission spectra in the region of 4.3 μm CO_2 band. These measurements were then used to retrieve vertical profiles of air temperature at 67 pressure levels in the Venusian mesosphere. The VIRTIS temperature sounding covers altitude range from 85 to 65 km (1–100 mbar). The overall error in retrieved temperature is<4 K in the range 100–0.1 mbar and is better than 1 K between 70 and 7 mbar. The main sources of errors and systematic uncertainties in the temperature retrievals are instrumental noise in the spectral ranges sounding high altitudes and uncertainties in the aerosols densities within the cloud deck (70–60 km) [*Grassi et al.*, 2008]. The VIRTIS observations analyzed in this work cover the night side in the southern hemisphere. The measurements on the day side have nonnegligible solar component and were excluded from our study.

[7] Figures 1 and 2 show example of the latitude-altitude temperature field retrieved from the VIRTIS-M observations in orbit 72 and corresponding latitude dependence of temperature at constant pressure levels. We used Chebyshev polynomials of degree 4 to fit the data points and to evaluate the latitudinal temperature gradient. Above 75 km (~20 mbar) temperatures on isobaric surfaces generally increase toward the pole. Below this level the temperature pattern becomes more complex and at 50°–70° latitude shows the region of temperature inversions at the cloud top (cold collar). In Figure 2 the cold collar is clearly visible as dip between 50° and 70° latitude at 40 and 90 mbar. Both positive temperature gradient in the higher mesosphere and cold collar right at the cloud tops were observed by Pioneer Venus [*Taylor et al.*, 1983; *Newman et al.*, 1984] and Venera-15 [*Zasova et al.*, 2007] missions in the northern hemisphere. VIRTIS observations in the south strongly suggest global hemispheric symmetry of the temperature field.

3. Zonal Thermal Winds

[8] Following *Newman et al.* [1984] we used cyclostrophic approximation to derive zonal wind pattern in the mesosphere from the VIRTIS temperature field. If we indicate with u the zonal wind speed in m/s, with $\zeta = -\ln(p/p_{ref})$ the logarithmic pressure vertical coordinate, with R the gas constant and with $(\partial T/\partial\phi)_{p\,=\,const}$ the latitudinal temperature gradient, it is possible to describe the zonal wind u by the thermal wind equation [*Schubert*, 1983]

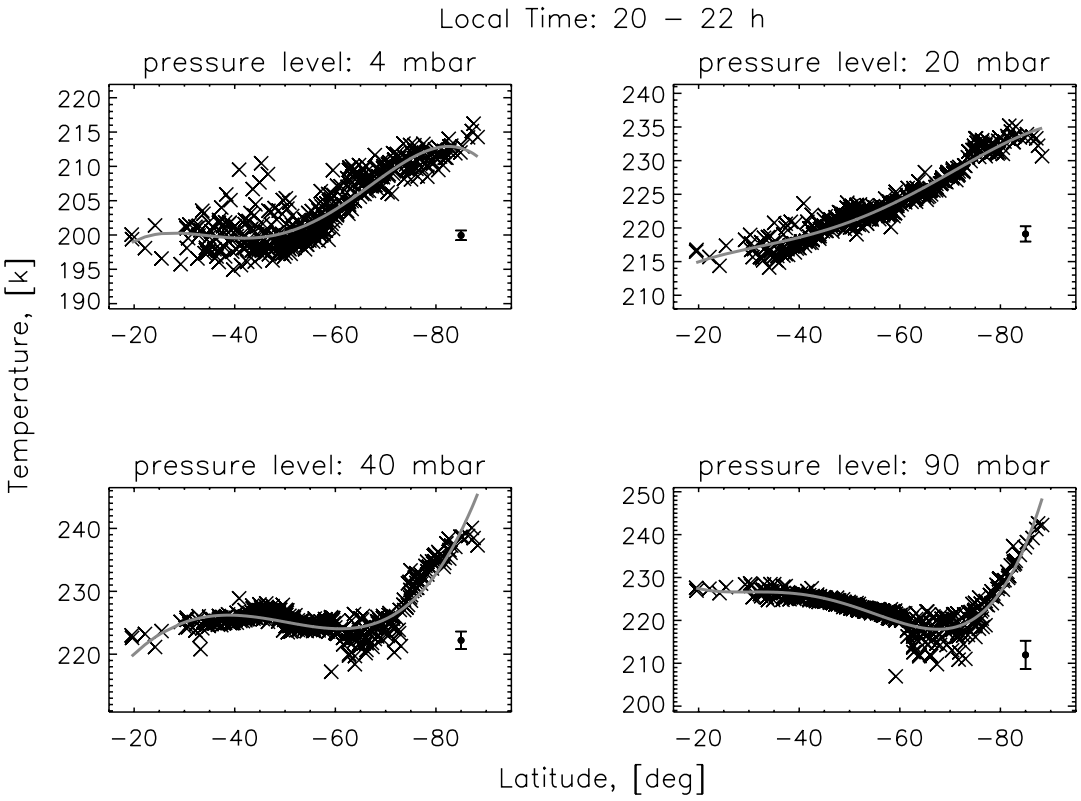

Figure 2. Plots of temperature at different pressure levels for 2000–2200 LT. Chebyshev polynomial approximation is represented in gray. Error bar shows random error of air temperature retrieval. Data refer to the VIRTIS-M orbit VI0072.

$$2u\frac{\partial u}{\partial \zeta} = -\frac{R}{\tan\phi}\frac{\partial T}{\partial \phi}\bigg|_{p=const} \qquad (1)$$

The retrieved air temperatures $T(\phi)$ were approximated by Chebyshev polynomials of degree 4 between 25° and 75° of latitude at 49 pressure levels. The lower boundary condition needed to solve differential equation (1) was

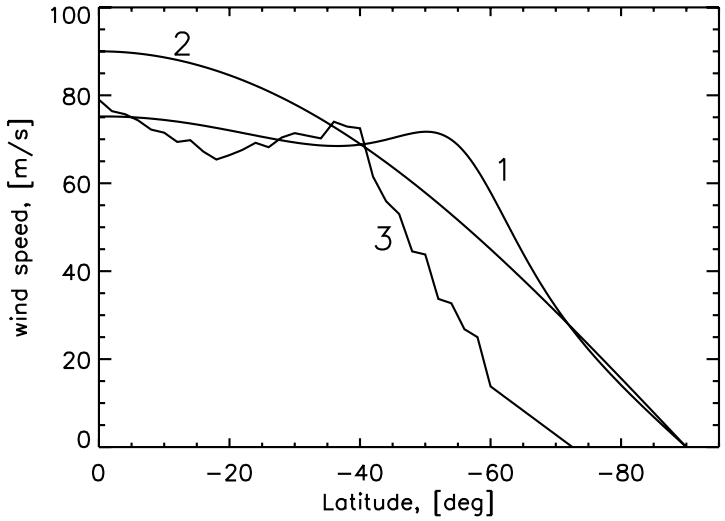

Figure 3. Functions used as lower boundary condition. Curve 1 is the function described by equation (2) used for the nominal case. Curve 2 is the solid body rotation function $u_0 = 90 \cos \phi$; as can be seen, it perfectly fits the curve 1 for latitudes higher than 70°, while at the equator it results 10 m/s stronger. Curve 3 represents the cloud-tracked wind derived from Galileo SSI NIR images [*Peralta et al.*, 2007]. This curve has the same magnitude of curve 1 near the equator, but a strong decrease in the wind speed is seen at latitudes higher than 40°.

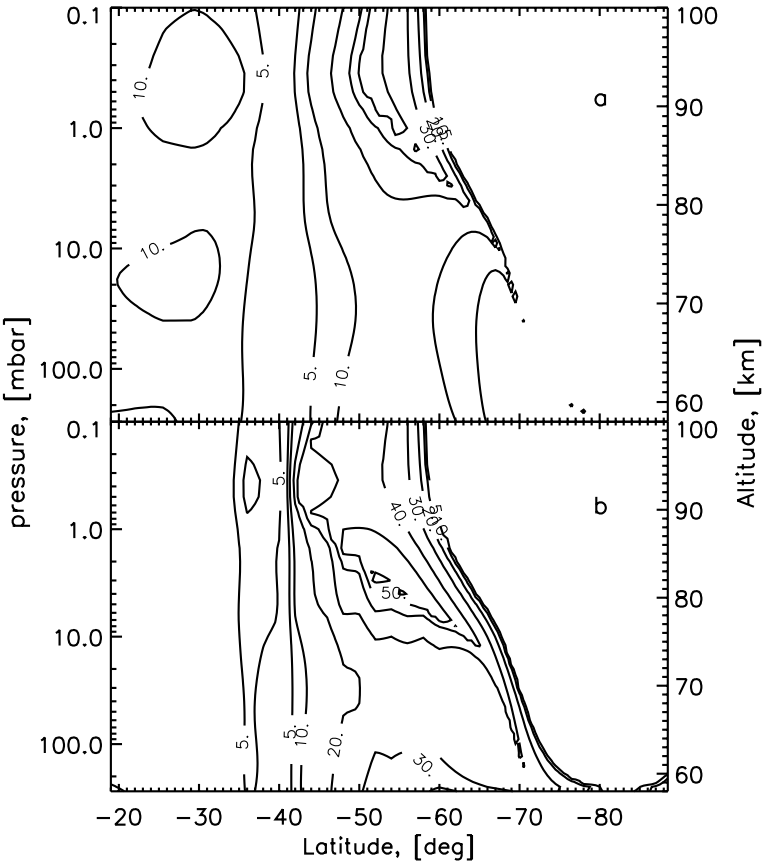

Figure 4. Contours of the difference absolute value (m/s) between the zonal thermal wind speed derived from VIRTIS temperature retrievals assuming $u_0 = (45 \sec h((\phi - 56)/9) + 75) \cos \phi$ as lower boundary condition and the zonal thermal wind derived assuming (a) $u_0 = 90 \cos\phi$ and (b) cloud-tracked winds derived from Galileo SSI NIR images as lower boundary condition. Data refer to the VIRTIS-M orbit VI0072.

taken at the reference pressure level p_{ref} = 275 mb (∼58 km) using the equation adopted by *Counselman et al.* [1980]; coefficients were selected to fit the Venus Monitoring Camera (VMC) direct measurements of wind profile and were provided by I. Khatuntsev (personal communications, 2008):

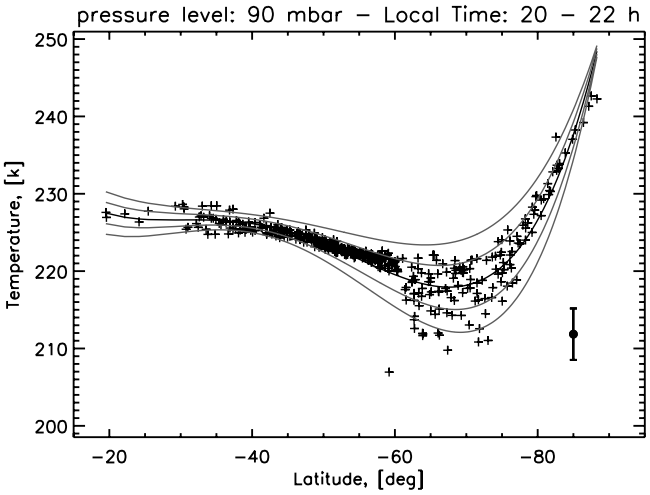

Figure 5. Latitude dependence of temperatures at a pressure level of 90 mb for 2000–2200 LT. Chebyshev polynomial approximation is represented in black together with the $\pm1\sigma$, $\pm2\sigma$ curves represented in gray. Error bar shows random error of air temperature retrieval. Data refer to the VIRTIS-M orbit VI0072.

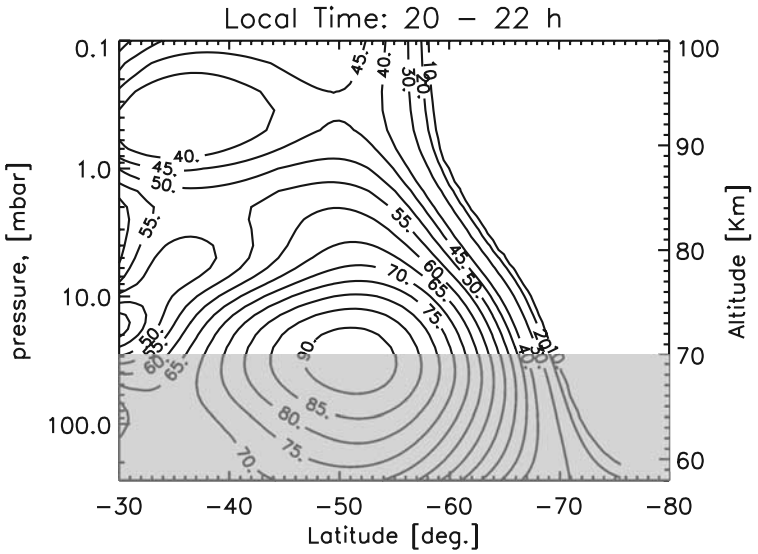

Figure 6. Contours of the zonal thermal wind speed (m/s) for 2000–2200 LT derived from VIRTIS temperature retrievals assuming cyclostrophic balance. Contour interval is 5 m/s. Data refer to the VIRTIS-M orbit VI0072. In gray the cloud layer is represented schematically.

$$U_0(\phi) = [45\,\mathrm{sech}((\phi - 56)/9) + 75]\cos\phi \qquad (2)$$

In order to test our retrieval code we used temperature field retrieved from Venera-15 Fourier Spectrometer (FS) data [*Zasova and Khatuntsev*, 1997]. Our test calculations were in good agreement with original results.

[9] We studied sensitivity of calculated thermal winds to numerical parameters and lower boundary conditions. First, we found that the Chebyshev polynomial of degree 4

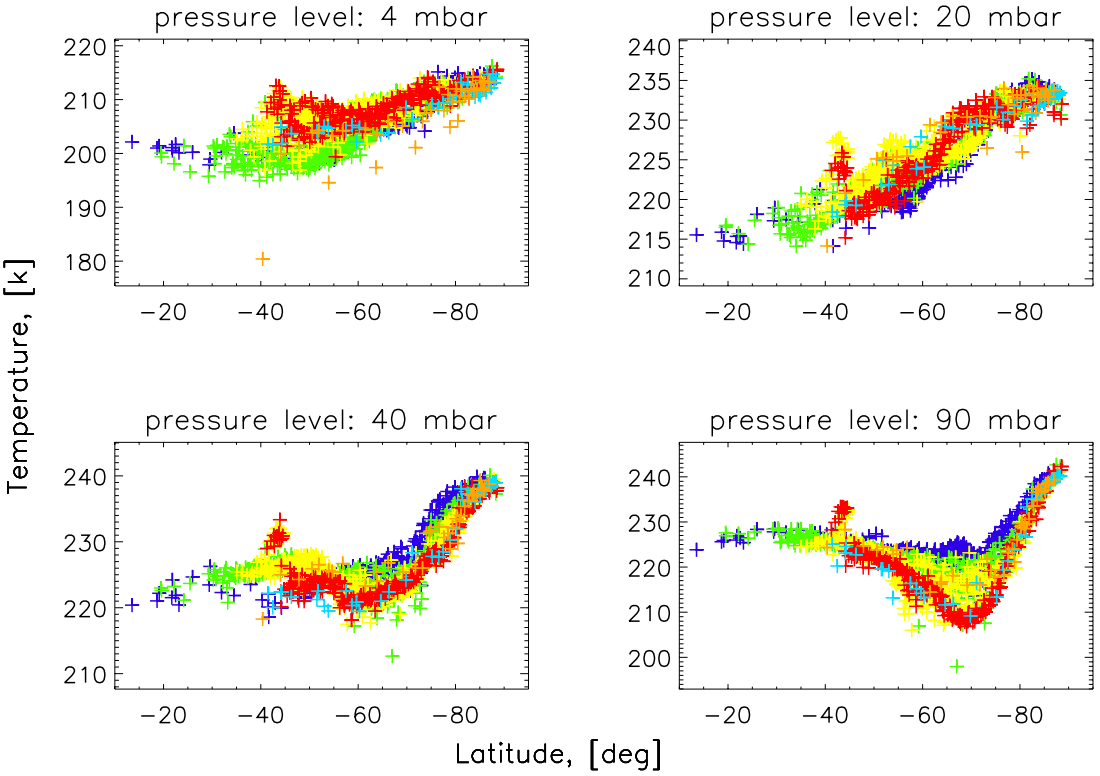

Figure 7. Plots of latitude dependence of temperatures at selected pressure levels; different colors correspond to different local time: (blue) 1800–2000 LT; (green) 2000–2200 LT; (yellow) 2200–2400 LT; (red) 0000–0200 LT; (light blue) 0200–0400 LT; and (orange) 0400–0600 LT. Data refer to the VIRTIS-M orbit VI0072.

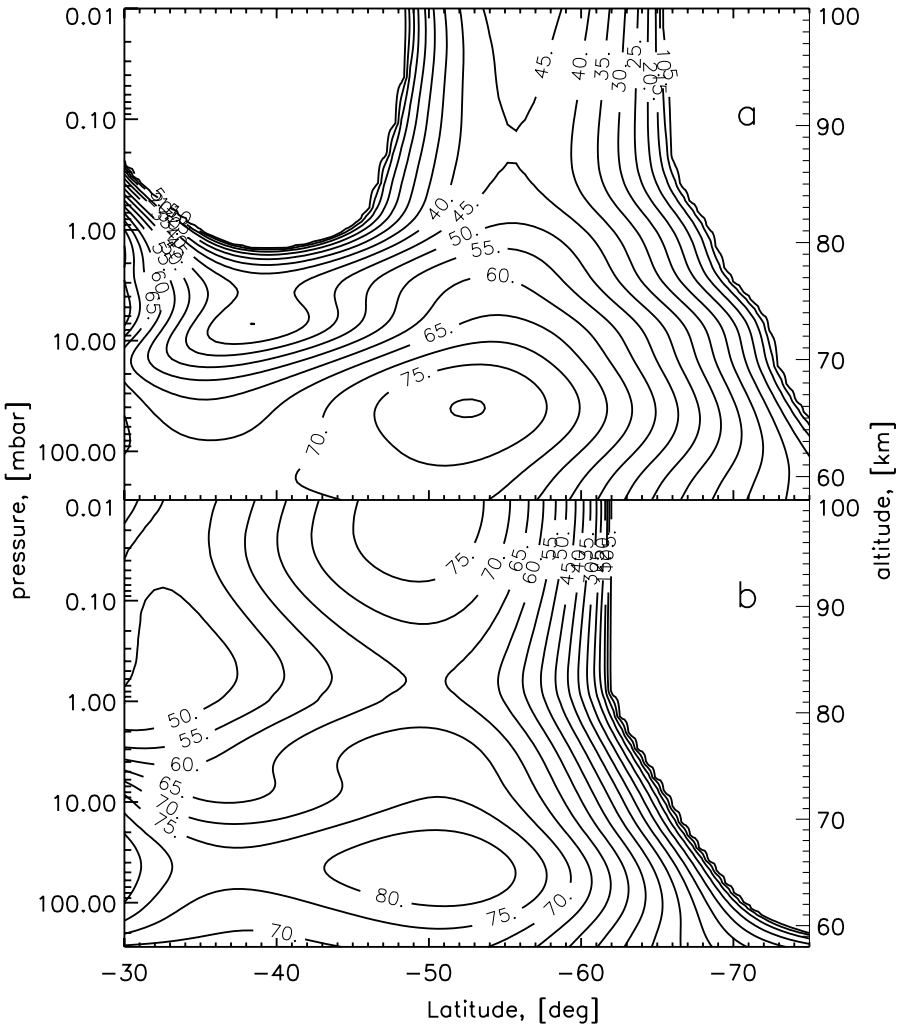

Figure 8. Contours of the zonal thermal wind speed (m/s) for (a) 1800–2000 LT and (b) 0300–0500 LT. Winds have been derived from VIRTIS temperature retrievals assuming cyclostrophic balance. Contour interval is 5 m/s. Data refer to 13 VIRTIS orbits acquired between May and December 2006.

provided the best fit to the data (Figure 2). Higher power of polynomial did not improve the data fit and resulted in high-frequency oscillations. Second, we considered different functions as lower boundary condition (Figure 3).

[10] We calculated the difference between the zonal wind field derived from VIRTIS temperature profiles using curve 1 as lower boundary condition and that obtained using curves 2 and 3 (Figures 4a and 4b). Both cases show small discrepancy with the nominal case (equation (2)) confirming that the retrieved wind weakly depends on the lower boundary condition. In Figure 4a the difference reaches maximum value of 40 m/s because of the absence in curve 2 of the midlatitude bulge present in curve 1 that forces winds to slow down with altitude faster than in the nominal case. In Figure 4b a bigger discrepancy is observed caused by the strong wind decrease at midlatitudes seen in Galileo NIR images. Both test cases show that lower boundary condition does not affect the region of the jet.

[11] Errors in the temperature retrievals are the source of uncertainty on the derived wind speed. We followed the approach used by *Newman et al.* [1984] to assess the propagation of temperature retrieval error on the wind field. On every pressure level air temperatures were averaged within 5° latitude bins. Mean value and standard deviation of each data point from approximating Chebyshev polynomial were calculated and centered in the interval. Another Chebyshev polynomial was used to fit the standard deviations and was added to the original polynomial approximation curve to produce the $+1\sigma$ curve. The -1σ and $\pm 2\sigma$ curves were calculated in a similar way. Figure 5 shows that almost all the data points are within $\pm 2\sigma$ range. Since scattering of the retrieved temperatures depends on latitude the gradients of $\pm 1\sigma$, $\pm 2\sigma$ curves differ from that of the original approximation curve that results in distortions of the wind field.

[12] Wind speeds were retrieved from $\pm 1\sigma$, $\pm 2\sigma$ curves, using equation (1) and the boundary conditions from equation (2) to assess the error in wind velocity determination. For all the curves, the position of the jet is not changed within 2° latitude. The wind field calculated for 1σ curve has a midlatitude jet speed of 89 m/s at 51° latitude. The speed of the jet for the 2σ curve is slightly altered. On the other hand for the -1σ and -2σ curves the speed of the jet reaches a value of 98 and 102 m/s

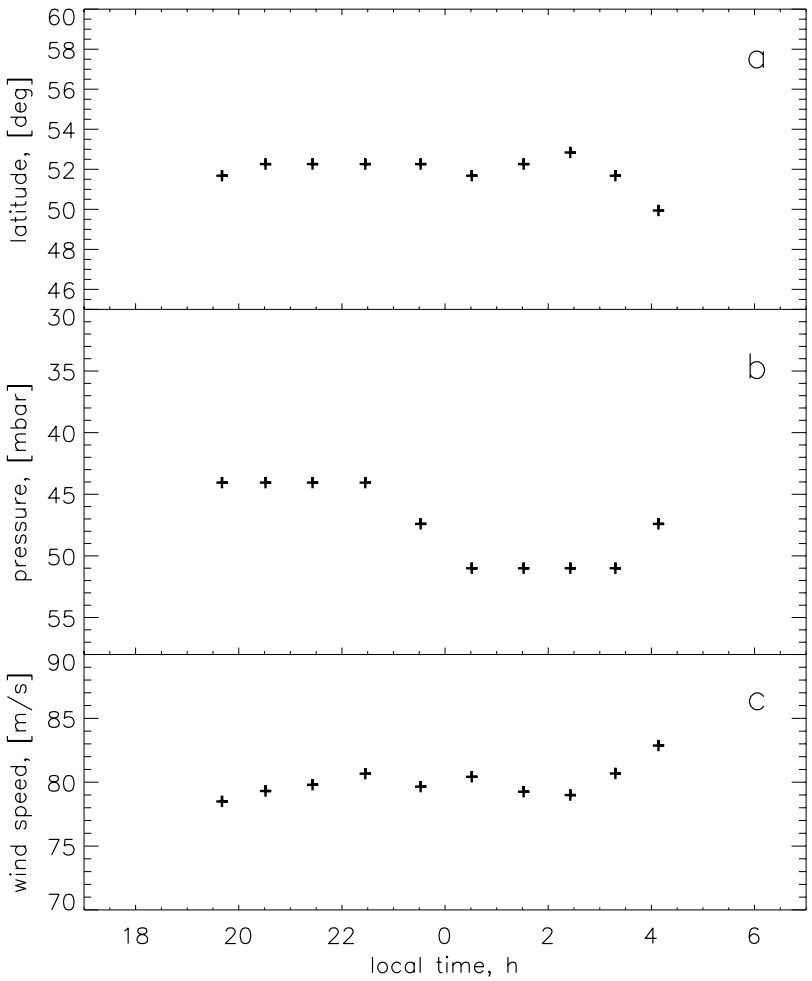

Figure 9. (a) Latitude of midlatitude jet versus local time for thirteen VIRTIS orbits acquired between May and December 2006; (b) Altitude of midlatitude jet versus local time; (c) Wind speed of midlatitude jet versus local time.

respectively. As an esteem of retrieval error on the midlatitude jet speed, it seems reasonable to take a value of ± 10 m/s which is comparable to the uncertainties on cloud-tracked winds derived from the Venus Monitoring Camera (R. Moissl et al., Cloud top winds from tracking UV features in VMC images, submitted to *Journal of Geophysical Research*, 2008).

[13] Figure 6 shows an example of thermal wind for 2000–2200 local time (LT) derived from the VIRTIS-M observations in orbit 72. The main feature in the plot is the midlatitude jet centered at 50° latitude and 67 km of altitude with a maximum speed of 90 m/s. Comparison of the wind field (Figure 6) with the temperature field (Figure 1) shows that the midlatitude jet is related to the cold collar.

[14] The thermal feature known as the warm polar mesosphere, characterized by an increase of temperature toward the pole on isobaric surfaces between 75 and 90 km of altitude, forces the retrieved zonal wind to decrease to zero very fast at higher latitudes. It is important to note, however, that for latitudes lower than 30° and higher than 75° the cyclostrophic balance fails, thus wind retrievals at these latitudes should not be taken in account.

[15] The VIRTIS observations in orbit 72 completely covered the night side of the southern hemisphere that allowed us to estimate the dependence of temperature field on local time. Figure 7 shows latitude profiles of temperatures at selected pressure levels for 2-h local time bins. They suggest that the atmosphere at the cloud tops cools down by about 15 K during the night. Theses changes in temperature structure also affect the thermal wind field.

[16] An example of the effect of diurnal variations of temperature structure is shown in Figures 8a and 8b. Wind field has been retrieved for two different local times combining the temperature profiles of thirteen VIRTIS orbits acquired between May and December 2006.

[17] Last, we examined in detail the dependence of the midlatitude jet on local time. Temperature profiles have been divided in local time intervals of 3 h and the wind speed has been retrieved for each local time bin. The behavior of midlatitude jet position and speed with local time has been analyzed in Figures 9a–9c. A change in the position and speed of the midlatitude jet can be clearly observed, however the magnitude of the variations lays within the uncertainties on retrieved wind speeds. There-

fore, any conclusion on local time dependence should be taken cautiously.

4. Discussion and Conclusions

[18] We presented the preliminary results of the cyclostrophic wind calculations from the VIRTIS-M temperature sounding in the southern hemisphere on the night side [*Grassi et al.*, 2008]. The main features of the wind field are (1) the presence of the midlatitude jet with peak velocity of 80–90 m/s centered at ~50°S at the cloud tops (~70 km); (2) fast decrease of zonal winds poleward from 60°S with zero velocity reached at ~70°S; and (3) gradual decrease of thermal wind with altitude above the jet. Our results are in general agreement with those based on the earlier observations [*Newman et al.*, 1984; *Zasova et al.*, 2007]. These features correlate with the behavior of the temperature field (Figure 1). According to the thermal wind equation (1) the negative latitude gradient within the upper cloud (<70 km) associated with the cold collar accelerates the wind. This trend changes with reversal of the temperature gradient above the cloud that causes thermal winds to fade out toward the top of the mesosphere. This deceleration is the strongest in high latitudes (>65°S) that results in that cyclostrophic balance breaks down in polar mesosphere (Figure 6).

[19] The magnitude of the jet in our results (80–90 m/s) is smaller than that reported by *Zasova et al.* [2007] (90–110 m/s) and especially by *Newman et al.* [1984] (140–160 m/s). This discrepancy can be partially attributed to the differences in numerical schemes and boundary conditions used in calculations, but seems to mainly result from peculiarities of temperature sounding techniques. Radio occultation data used by *Newman et al.* [1984] provide temperature structure with vertical resolution of few hundred meters that allows the measurements to completely resolve deep temperature inversions typical for the cold collar regions. Vertical resolution in thermal emission spectroscopy in the CO_2 bands used by *Zasova et al.* [2007] and in this work does not exceed few kilometers. This smoothes temperature inversions and effectively reduces the latitudinal gradient of temperature that eventually accelerates the wind.

[20] Comparison of the thermal wind field to the cloud-tracked winds is the test bench for cyclostrophic balance assumption. Results of our calculations in first order agree with the Venus Express measurements of the cloud top winds [*Sanchez-Lavega et al.*, 2008; R. Moissl et al., submitted manuscript, 2008] that gave the wind speed of 80–100 m/s at ~50°S and fast decrease of zonal wind poleward. However, our thermal wind deviates from the observed one in low latitudes (<40°S), indicating that cyclostrophic balance is not valid here. The core of the cyclostrophic jet is located almost exactly at the cloud tops (~70 km) in all thermal wind calculations. We note, however, that the latitudinal profiles of thermal wind at this altitude have much sharper maxima than those observed in cloud-tracked winds.

[21] Following the earlier studies, especially the one by *Zasova et al.* [2007], we searched for local time variability in the properties of the midlatitude jet. The temperature field clearly indicates radiative cooling by ~15 K of the night side atmosphere at the cloud tops (Figure 7) which also propagates to the thermal wind field (Figures 9a–9c). However, we prefer to be cautious in making conclusions on this basis. First, the coverage by VIRTIS temperature sounding that we used so far is limited by the night side. And, second and probably more important, the weak meandering of the thermal wind field of 10–20 m/s that results from diurnal variations of temperature structure seems to be within the "ignorance" range of the cyclostrophic hypothesis itself. For instance, the equation (1) was derived ignoring the meridional wind component which is of ~15 m/s. So there could be some doubt that the wind field variations of 10–20 m/s, although derived by correct numerical procedures, are physically meaningful.

[22] The future work will include the use of VIRTIS temperature sounding extended to the northern hemisphere and the day side. This would allow us to better constrain the thermal wind at 20°–40°S and to extend the coverage to the northern hemisphere and to study hemispheric symmetry of the wind field. Days side temperature sounding would be needed to complete local time coverage and would allow comparison with simultaneously derived cloud-tracked winds. And, finally, extensive radio occultation sounding by VeRa/Venus Express would allow the thermal wind calculations to be extended to as deep as 40 km. Comparison of the thermal wind field derived from the combined VIRTIS/VeRa temperature structure with the winds derived from cloud features tracking in UV (~70 km) and near IR on the night side (~50 km) would eventually allow one to conclude about the regions of validity of the cyclostrophic balance.

[23] **Acknowledgments.** We thank S. Limaye for fruitful discussions of the results. A. Piccialli is grateful to the Max Planck Research School for providing the opportunity to carry out this study. VIRTIS-Venus Express is an experiment developed jointly by IASF-INAF (Italy) and LESIA, Observatoire de Paris (France). The project is funded by ASI and CNES.

References

Bougher, S. W., M. J. Alexander, and H. G. Mayr (1997), Upper atmosphere dynamics: Global circulation and gravity waves, in *Venus II*, edited by S. W. Bougher, et al., pp. 259–291, Univ. of Ariz. Press, Tucson.

Chub, E. V., and O. I. Yakovlev (1980), Temperature and zonal circulation of the atmosphere of Venus based on the data of radio probe experiments, *Cosmic Res., Engl. Transl.*, *18*, 331–336.

Counselman, C. C., S. A. Gourevitch, R. W. King, G. B. Loriot, and E. S. Ginsberg (1980), Zonal and meridional circulation of the lower atmosphere of Venus determined by radio interferometry, *J. Geophys. Res.*, *85*, 8026–8030, doi:10.1029/JA085iA13p08026.

Drossart, P., et al. (2007), Scientific goals for the observation of Venus by VIRTIS on ESA/Venus Express mission, *Planet. Space Sci.*, *55*, 1653–1672, doi:10.1016/j.pss.2007.01.003.

Gierasch, P., et al. (1997), The general circulation of the Venus atmosphere: An assessment, in *Venus II*, edited by S. W. Bougher, et al., pp. 459–500, Univ. of Ariz. Press, Tucson.

Grassi, D., P. Drossart, G. Piccioni, N. I. Ignatiev, L. V. Zasova, A. Adriani, M. L. Moriconi, P. G. J. Irwin, A. Negrao, and A. Migliorini (2008), Retrieval of air temperature profiles in the Venusian mesosphere from VIRTIS-M data: Description and validation of algorithms, *J. Geophys. Res.*, *113*, E00B09, doi:10.1029/2008JE003075.

Häusler, B., et al. (2006), Radio science investigations by VeRa onboard the Venus Express spacecraft, *Planet. Space Sci.*, *54*, 1315–1335, doi:10.1016/j.pss.2006.04.032.

Lellouch, E., T. Clancy, D. Crisp, A. Kliore, D. Titov, and S. Bougher (1997), Monitoring of mesospheric structure and dynamics, in *Venus II*, edited by S. W. Bougher, et al., pp. 295–324, Univ. of Ariz. Press, Tucson.

Leovy, C. B. (1973), Rotation of the upper atmosphere of Venus, *J. Atmos. Sci.*, *30*, 1218–1220, doi:10.1175/1520-0469(1973)030<1218:ROTUAO>2.0.CO;2.

Limaye, S. S. (1985), Venus atmospheric circulation: Observations and implication of the thermal structure, *Adv. Space Res.*, *5*, 51–62, doi:10.1016/0273-1177(85)90270-4.

Newman, M., G. Schubert, A. J. Kliore, and I. R. Patel (1984), Zonal winds in the middle atmosphere of Venus from Pioneer Venus radio occultation data, *J. Atmos. Sci.*, *41*, 1901–1913, doi:10.1175/1520-0469(1984)041<1901:ZWITMA>2.0.CO;2.

Peralta, J., R. Hueso, and A. Sánchez-Lavega (2007), A reanalysis of Venus winds at two cloud levels from Galileo SSI images, *Icarus*, *190*(2), 469–477, doi:10.1016/j.icarus.2007.03.028.

Piccioni, G., et al. (2008), *VIRTIS (Visible and Infrared Thermal Imaging Spectrometer) for Venus Express*, Eur. Space Agency, Noordwijk, Netherlands, in press.

Roos-Serote, M., P. Drossart, T. Encrenaz, E. Lellouch, R. W. Carlson, K. H. Baines, F. W. Taylor, and S. B. Calcutt (1995), The thermal structure and dynamics of the atmosphere of Venus between 70 and 90 km from the Galileo-NIMS spectra, *Icarus*, *114*(2), 300–309, doi:10.1006/icar.1995.1063.

Sanchez-Lavega, A., et al. (2008), Variable winds on Venus mapped in three dimensions, *Geophys. Res. Lett.*, *35*, L13204, doi:10.1029/2008GL033817.

Schubert, G. (1983), General circulation and the dynamical state of the Venus atmosphere, in *Venus*, edited by D. M. Hunten, et al., pp. 651–765, Univ. of Ariz. Press, Tucson.

Schubert, G., S. W. Bougher, C. C. Covey, A. D. Del Genio, A. S. Grossman, J. L. Hollingsworth, S. S. Limaye, and R. E. Young (2007), Venus atmosphere dynamics: A continuing enigma, in *Exploring Venus as a Terrestrial Planet*, *Geophys. Monogr. Ser.*, vol. 176, edited by L. W. Esposito, E. R. Stofan, and T. E. Cravens, pp. 121–138, AGU, Washington, D. C.

Seiff, A. (1983), Thermal structure of the atmosphere of Venus, in *Venus*, edited by D. M. Hunten, et al., pp. 215–279, Univ. of Ariz. Press, Tucson.

Seiff, A., J. T. Schofield, A. J. Kliore, F. W. Taylor, S. S. Limaye, H. E. Revercomb, L. A. Sromovsky, V. V. Kerzhanovich, V. I. Moroz, and M. Y. Marov (1985), Models of the structure of the atmosphere of Venus from the surface to 100 kilometers, *Adv. Space Res.*, *5*, 3–58, doi:10.1016/0273-1177(85)90197-8.

Svedhem, H., et al. (2007), Venus Express—The first European mission to Venus, *Planet. Space Sci.*, *55*, 1636–1652, doi:10.1016/j.pss.2007.01.013.

Taylor, F. W., D. M. Hunten, and L. V. Ksanfomaliti (1983), The thermal balance of the middle and upper atmosphere of Venus, in *Venus*, edited by D. M. Hunten, et al., pp. 650–680, Univ. of Ariz. Press, Tucson.

Titov, D. V., et al. (2006), Venus Express science planning, *Planet. Space Sci.*, *54*, 1279–1297, doi:10.1016/j.pss.2006.04.017.

Zasova, L. V., and I. V. Khatuntsev (1997), Thermal zonal wind in the Venus middle atmosphere according to Venera 15 IR-spectrometry, *Adv. Space Res.*, *19*, 1181–1190, doi:10.1016/S0273-1177(97)00269-X.

Zasova, L. V., N. Ignatiev, I. Khatuntsev, and V. Linkin (2007), Structure of the Venus atmosphere, *Planet. Space Sci.*, *55*, 1712–1728, doi:10.1016/j.pss.2007.01.011.

P. Drossart, LESIA, Observatoire de Paris, Section de Meudon, 5 place Jules Janssen, F-92195 Meudon, France.

D. Grassi, Istituto di Fisica dello Spazio Interplanetario, INAF, Via del Fosso del Cavaliere 100, I-00133 Rome, Italy.

I. Khatuntsev, Space Research Institute, 84/32 Profsojuznaja Str, 117997 Moscow, Russia.

A. Migliorini and G. Piccioni, Istituto di Astrofisica Spaziale e Fisica Cosmica, INAF, Via del Fosso del Cavaliere 100, I-00133 Rome, Italy.

A. Piccialli and D. V. Titov, Max Planck Institute for Solar System Research, Max Planck Strasse 2, D-37191 Katlenburg-Lindau, Germany.